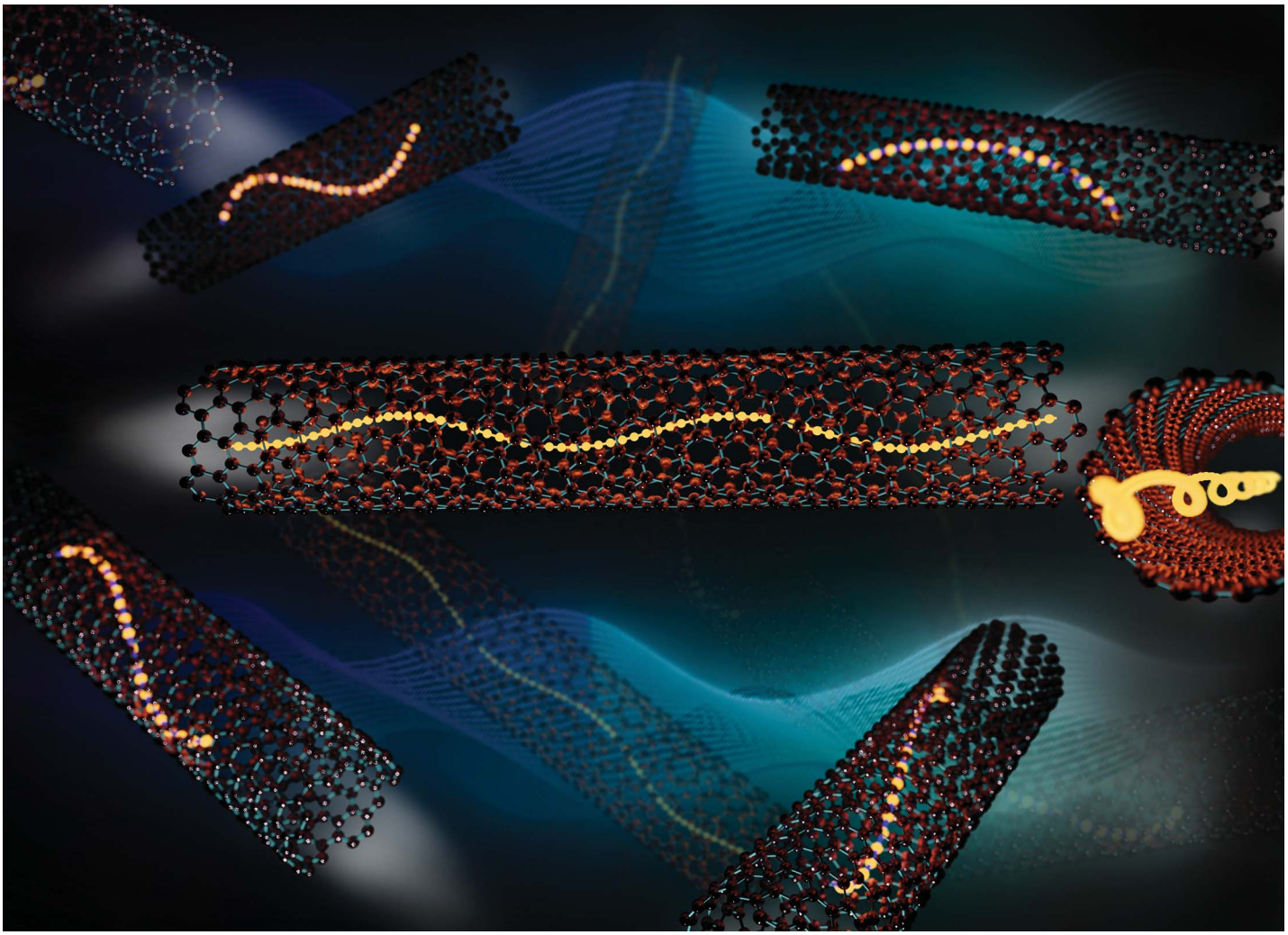

Showcasing research from Professor Guy Makov's laboratory, Dept. of Materials Engineering, Ben-Gurion University of the Negev, Israel.

Carbon nanowires under compression and their vibrational anomalies

Carbon nanowires are shown to be dynamically unstable under compression through *ab initio* phonon spectra calculations. To stabilise nanowires under compression they transform from linear forms to two-dimensional sinusoidal shapes. If encapsulated in carbon nanotubes, they can further transform to novel three-dimensional helical forms. These results are demonstrated using density functional based quantum, classical atomistic and continuum modelling approaches.

As featured in:

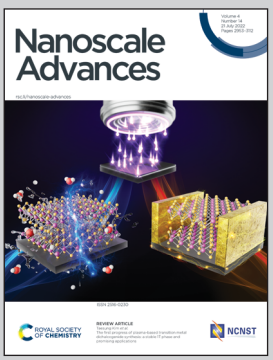

See Uri Argaman and Guy Makov, *Nanoscale Adv.*, 2022, **4**, 2996.

ROYAL SOCIETY OF CHEMISTRY

rsc.li/nanoscale-advances

Registered charity number: 207890

Nanoscale Advances

ROYAL SOCIETY OF CHEMISTRY

PAPER

View Article Online
View Journal | View Issue

Cite this: *Nanoscale Adv.*, 2022, **4**, 2996

Carbon nanowires under compression and their vibrational anomalies†

Uri Argaman[a] and Guy Makov *[ab]

Anomalous pressure dependence of Raman frequencies of carbon nanowires encapsulated in carbon nanotubes has been recently reported. Two hypotheses have been proposed to explain this phenomenon in linear carbon chains: softening of a carbon bond with pressure or charge transfer to the chain. However, carbon chains bend easily under stress, although stable structures under these conditions have yet to be discovered. In this study, we model linear and bent carbon nanowires under compression, including both stable and metastable structures. The structures, electronic properties, and vibrational frequencies are obtained through first-principles calculations within density functional theory. We find that polyyne, the dimerized linear ground-state structure of carbon chains at zero strain, is not stable under compression for an infinite carbon chain. Instead, the chain transforms into two possible configurations, a previously unknown three-dimensional helical shape or a two-dimensional sinusoidal shape. These structures can be modeled using an analytical atomistic force-constant model or with a continuum approach. In the continuum approach, an eigenvalue wave equation describes the energy and geometry of the chain. Moreover, this equation produces excited (metastable) structural states and can be applied to other one-dimensional systems. The wave equation formulation indicates that the much-pursued concept of Young's modulus in one-dimensional chains is ill-defined. Finally, the Raman anomaly under compression is not observed within the atomistic force-constant model contrary to assumptions in the literature. Instead, this anomaly can be understood using a model in which charge transfer between the nanotube and the nanowire occurs upon contact.

Received 11th January 2022
Accepted 17th May 2022

DOI: 10.1039/d2na00027j

rsc.li/nanoscale-advances

Atomic carbon wires, denoted as carbynes, are idealized, infinitely long carbon chains. Carbynes can be naturally found (*e.g.* in meteorites), but, in most cases, they are synthesized in a laboratory with finite length.[1] There are two common finite chain allotropes:[2] polyynes, with alternating single and triple carbon bonds reflected in alternating bond lengths, and cumulenes, which have one repeated double bond.[1] The properties of these carbon chain structures are currently under intensive study[1,3–7] along with their potential applications, such as nanoelectronics, spintronics, and nonlinear optics.[1,4,5]

Carbon chains can be synthesized in solution with lengths of tens of atoms before being crystallized.[1] However, because of their strong reactivity, protecting them is necessary, *e.g.*, with specific end-groups.[1] As an alternative form of protection, carbon chains can be encapsulated in carbon nanotubes (CNTs),[3,5] which can stabilize much longer carbon chains of up to 6000 atoms and 600 nm.[5]

The structure of linear carbon chains has been modeled through first-principles calculations in several studies.[3,4,8] Their stable structure at low temperatures was found to be linear (polyyne) with semiconductor properties. The cumulene structure was found to be unstable with semimetallic properties. Under tension, bond length alternation (BLA) increased with strain, stabilizing the polyyne structure.[9] Strain energy was found to be representable by a simple analytical atomistic force-constant model. The mechanical stability of finite polyyne chains has been considered within a continuum-mechanics-based model, and they were found to buckle beyond a critical compressive strain.[10] Several studies have attempted to evaluate Young's modulus of carbon chains, leading to an unusually wide range of predicted values across two orders of magnitude between 0.3 and 32.7 GPa.[11,12] The extremely large value of 32.7 GPa, approximately 32 times larger than Young's modulus of diamond, was obtained from a calculation of the tensile and bending stiffness.[12] Using this approach, the authors calculated the chain radius to be 0.386 Å, which is much smaller than ~0.7 Å, the atomic radius of carbon.

Chain length, *via* calculations, has been found to affect polyyne material properties strongly. In particular, increasing

[a]*Materials Engineering Department, Ben-Gurion University of the Negev, Beer Sheva 84105, Israel. E-mail: makovg@bgu.ac.il*

[b]*Ilse Katz Institute for Nanoscale Science and Technology, Ben-Gurion University of the Negev, Beer-Sheva 84105, Israel*

† Electronic supplementary information (ESI) available: Mathematical derivation of the dispersion relation of both chains with one type of bond and two types of bonds; the derivation of the wave equation in the continuum approach; the derivation of the formula for the energy in the continuum approach. See https://doi.org/10.1039/d2na00027j

the chain length has been shown to reduce the BLA between single and triple carbon bonds, reduce the highest occupied molecular orbital (HOMO)–lowest unoccupied molecular orbital (LUMO) gap,[4,5] and decrease the Raman frequency associated with the vibrations of the triple bond.[13,14] All these phenomena can be understood by the increasing conjugation of the bonds with increasing polyyne length. However, it is assumed that these effects converge before a transition into a cumulene structure that has zero BLA and no bandgap.[6]

Recently, several studies compressed carbon chains encapsulated in CNTs under hydrostatic pressure inside diamond anvil cells and measured the Raman spectra of the chains.[11,15,16] In these studies, an anomaly was observed, as the Raman frequency decreased with increasing pressure, *i.e.*, it had a negative Grüneisen parameter. Two hypotheses have been put forward to explain this observation. The first is bond softening with pressure; for example, in ref. 11, the authors interpreted that the experimental Raman frequency softening corresponds to single-carbon-bond softening under pressure. The second hypothesis suggested that the softening can be attributed to the charge transfer from the CNT to the carbon chain.[15]

All these analyses assumed that the carbon chain was linear. However, it is well known that carbon chains are easily distorted from their linear form to become bent either because of the material environment, *e.g.*, upon crystallization or external loading.[17] The effects of bending on the structure have been examined;[18,19] and the deviation of bond angles from 180° increases with the arc–chord ratio. The bending energy can be analytically modeled, in which a bending term with a single parameter is added to the standard harmonic terms.[18] Several experimental and theoretical studies on the structure of bent carbon chains have shown that Raman frequency decreases with chain bending.[18,19] Thus, a third hypothesis may be proposed stating that the bending of the carbon chains causes the observed decrease in the Raman frequency under pressure. However, the conditions for carbyne bending and for the stability of linear and bent chains have not been determined.

This study investigates the structure, stability, and Raman frequencies of linear and bent carbon chains by calculating the total energy and phonon spectra through first-principles based density functional theory (DFT). First, we show that the phonon spectrum of a linear chain exhibits imaginary frequencies under compression, indicating mechanical instability. The strain at which the instability presents itself is found to be dependent on chain length. Introducing random displacements in two and three dimensions and then minimizing the energy reveals that compressed carbon chains have either a two-dimensional sinusoidal form or a three-dimensional helical form. The bent chain structures' phonon frequencies and their strain dependence are calculated, and they indicate that the chains are dynamically stable. Subsequently, an atomistic model to describe the chain energy as a function of strain and shape is formulated. We find the conditions necessary for the stability of both finite and infinite strained linear chains, as well as the pressure dependence of the bond force constants. This model is reformulated in the continuum limit as an eigenvalue wave-equation to provide additional insight into one-dimensional chains and indicates that the concept of Young's modulus is irrelevant in one-dimensional chains. Finally, the effect of charge transfer on the aforementioned phonon spectra is considered. We conclude with a discussion on the stability of carbon chains and other one-dimensional atomic structures when compressed as well as the origin of the anomalous Raman shift under pressure.

Results and discussion

Phonon spectrum of a linear chain under strain

In the absence of strain and at 0 K, our density functional calculations predict that the infinite linear chain has a dimerized structure. The two-atom unit cell has bond lengths of 1.26 and 1.30 Å, which are in excellent agreement with the experimental limiting values as the chain length increases to infinity.[1]

The phonon spectrum of a linear chain with a two-atom unit cell was calculated as a function of strain relative to the equilibrium state, and the results are presented in Fig. 1(a). The longitudinal acoustic and optical branches present high frequencies, while the transverse branches present low frequencies. The frequencies of the longitudinal acoustic branch cross over the transverse optical branch at short wavelengths. At zero strain, all the phonon frequencies are positive, and the chain is stable. This stable condition persists under tension (positive strain). The change in phonon frequencies, ω, with uniaxial strain, ε, can be represented by uniaxial mode Grüneisen parameters, which are defined as follows:

$$\gamma_\varepsilon \equiv -\frac{1}{\omega} \times \frac{\partial \omega}{\partial \varepsilon}. \quad (1)$$

We found that in the linear chain, both of the transverse branches have negative values of γ_ε at all wavelengths, as opposed to the longitudinal branches, which had positive γ_ε values.

Consequently, upon compression, *i.e.*, negative strain, the infinite chain is dynamically unstable, with imaginary frequencies appearing in the transverse acoustic branch, as seen in Fig. 1(a). The imaginary frequencies signify that the linear chain is not a local minimum of the Born–Oppenheimer potential energy surface and that atomic displacements perpendicular to the chain direction, *i.e.*, bending deformations, reduce the energy. The phonon spectra under tension can be measured in principle, whereas those calculated under compression have no physical meaning in the experiments because they describe a mechanically unstable structure.

The structure of the chain under strain bending

As the infinite linear chain is not stable under compression, another stable structure must exist, which can be found by minimizing the total energy subject to suitable constraints and initial conditions in either two or three dimensions. We found two mechanically stable structures for the infinite chain: a two-dimensional sinusoidal structure in which all the atoms are on the same plane and a three-dimensional helical structure.

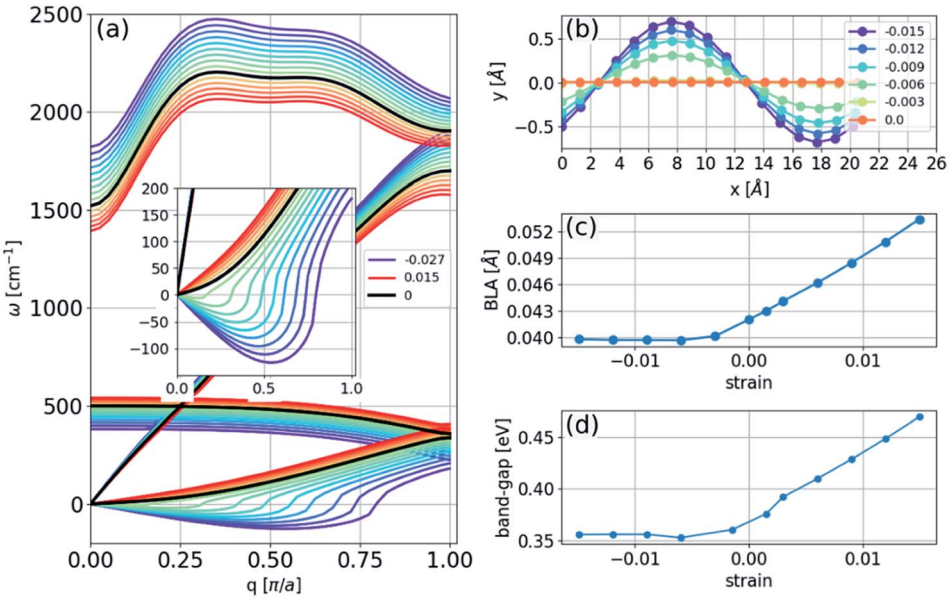

Fig. 1 (a) Phonon spectra of a linear carbon chain with a two-atom unit cell calculated at several strains; inset: a detailed view of the long-wavelength limit of the spectrum; legend: zero and extremal strains; the strain difference between every two adjacent curves is 0.003. (b–d) The calculated relaxed chain geometry and electronic structure in a 16-atom unit cell: (b) several strains under compression as denoted in the legend; (c) BLA; and (d) bandgap as a function of strain.

The two-dimensional structure

To obtain the structure of an infinite chain in two dimensions, we considered unit cells of varying sizes (2 to 16 atoms in length) with PBC and introduced random displacements in two dimensions. The result of the energy minimization of the chain is a sinusoidal structure with larger amplitudes at larger strains, as illustrated in Fig. 1(b). The BLA increased in magnitude under tension, decreasing under compression until it reached a nonzero limiting value of 0.040 Å (Fig. 1(c)). This result implies that the polyyne structure remains energetically favorable even under compression, and a transition to a cumulene structure does not occur. Thus, no insulator-metal transition will occur under pressure, as shown in Fig. 1(d), which can be understood because the bandgap is correlated with the BLA (Peierls transition).

Finite two-dimensional chains

The sinusoidal structure of the infinite chain, as shown in Fig. 1, is determined by the PBC employed in the calculations and may be a good approximation for long chains. However, in experiments, chains have a finite length that can be just a few atoms long. To study the structure of finite chains under compression, we considered a chain of 16 carbon atoms terminated with a hydrogen atom at each end. The choice of termination group can affect the electronic structure and determine whether the stable structure is a polyyne or cumulene,[9] but it is not expected to have a considerable effect on bending properties. As a demonstration we calculated the bending of a 16-atom carbon chain terminated either with a single hydrogen atom or two hydrogens at each end. The result is shown in Fig. 2(e) and it can be seen that the difference between the two chains is not significant. To obtain the minimum energy structure, we initiated the relaxation process from a linear structure with random displacements of the atoms in two directions and found an arc-like structure (Fig. 2). The compression has almost no effect on the bond lengths (Fig. 2(d)). As the compressive strain is increased, the amplitude of the arc increases. If the environment geometrically constrains the chain, limiting the amplitude of the arc (*e.g.*, packing the chains into an array or encapsulating in CNTs), this structure will no longer be accessible, leading to a three-dimensional structure.

Three-dimensional structure – the helix

If the energy of the carbon chain is minimized after introducing random atomic displacements in three dimensions instead of two, we then obtain a novel class of three-dimensional helical structures. We consider unit cells of varying sizes from 8 to 28 atoms in length with PBC at constant strain. We find that the three-dimensional structure of a carbon chain under pressure, determined by total energy minimization, is helical (Fig. 3) that can be described as follows:

$$x_n = \mathrm{int}\left(\frac{n+1}{2}\right)\Delta x_1 + \mathrm{int}\left(\frac{n}{2}\right)\Delta x_2, \quad (2)$$

$$y_n = A\,\sin(k_y x_n), \quad (3)$$

$$z_n = A\,\cos(k_z x_n), \quad (4)$$

where x is the periodic direction. x_n, y_n, and z_n are the components of the positions of the atoms; A is an amplitude determined by the strain; Δx_1 and Δx_2 are the two projections of the bond distances on the x-axis, and int(Q) denotes the integer part of Q. If $k_y = k_z$, this structure is a helix with a circular cross-

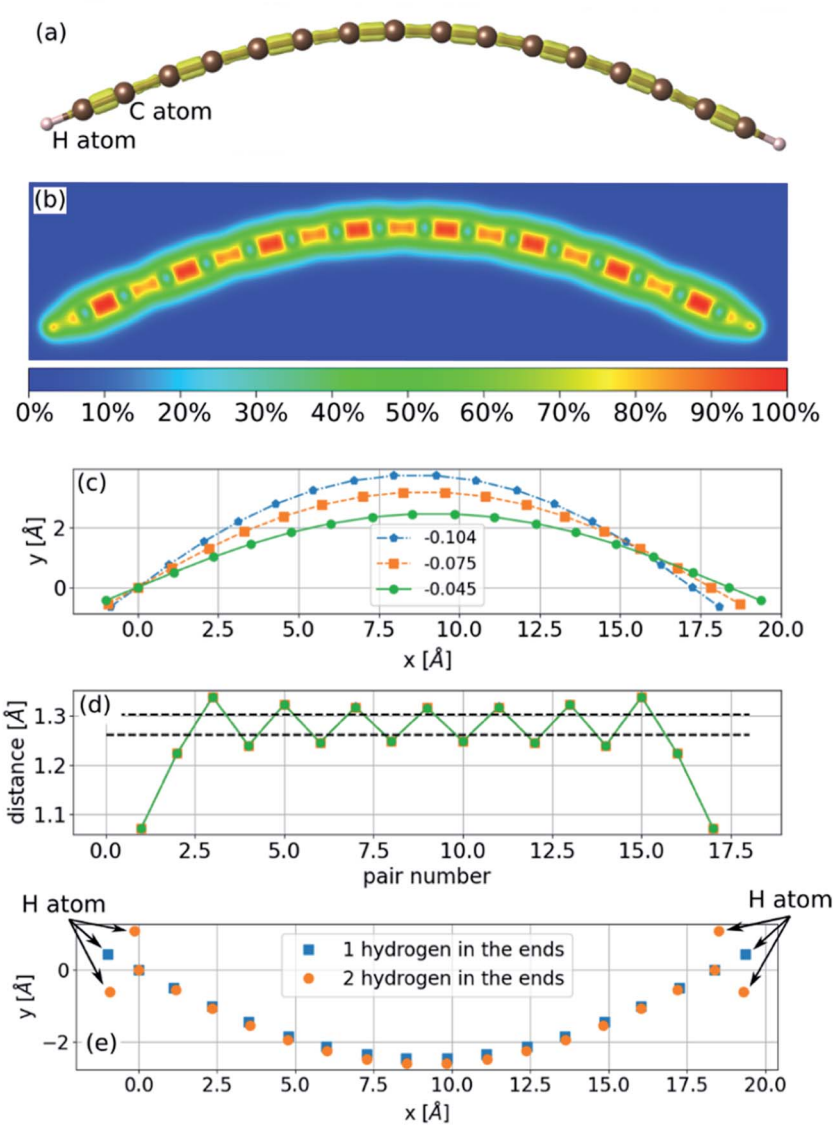

Fig. 2 The structure of a finite chain with 16 carbon atoms terminated with two hydrogen atoms. (a and b) Under a strain of −0.045; the isosurface in (a) is 75% of the maximal density, and the color map in (b) represents the density, (c) the geometry of the chain under several strains as shown in the legend; (d) the distances between neighboring atoms in the chain; dashed black lines mark the nearest neighbor distance at zero strain in the infinite chain; (e) the geometry of the chain with one and two hydrogens atoms at the ends at strain of −0.03. Arrows point to the hydrogen atoms and all the other atoms are carbon.

section (Fig. 3(b)), and the bond angles are approximately constant (Fig. 3(c)). These angles approach 180° as the chain length increases, as shown in Fig. 3(c). We note that, in general, k_y can take on a different value than k_z. Previously, a three-dimensional helix structure has been observed in iodine chains inside CNT and confirmed by DFT calculations.[20] However, the formation of the helix there was dominated by interaction between the chain and the surrounding CNT.

Comparison between two- and three-dimensional structures

The two- and three-dimensional structures are both local minima of the Born–Oppenheimer potential energy surface (mechanically stable structures) for a fixed number of atoms. As expected, the three-dimensional structure has a slightly lower energy per atom due to the additional degree of freedom (Fig. 3(e)). The bond lengths are approximately constant in two- and three-dimensional structures and gradually become similar to the relaxed bond lengths of the chain. In contrast, the bond angles of the three-dimensional helical structure are approximately constant, whereas those of the two-dimensional sinusoidal structure exhibit considerable variation (Fig. 3(d)). This difference suggests that additional stabilization of the three-dimensional structure is obtained by reducing the bonds' angular contribution to the energy.

Phonon normal modes of the bent two-dimensional structure

To find the vibrational properties of the carbyne chain under compression, the optical phonon frequencies are calculated at

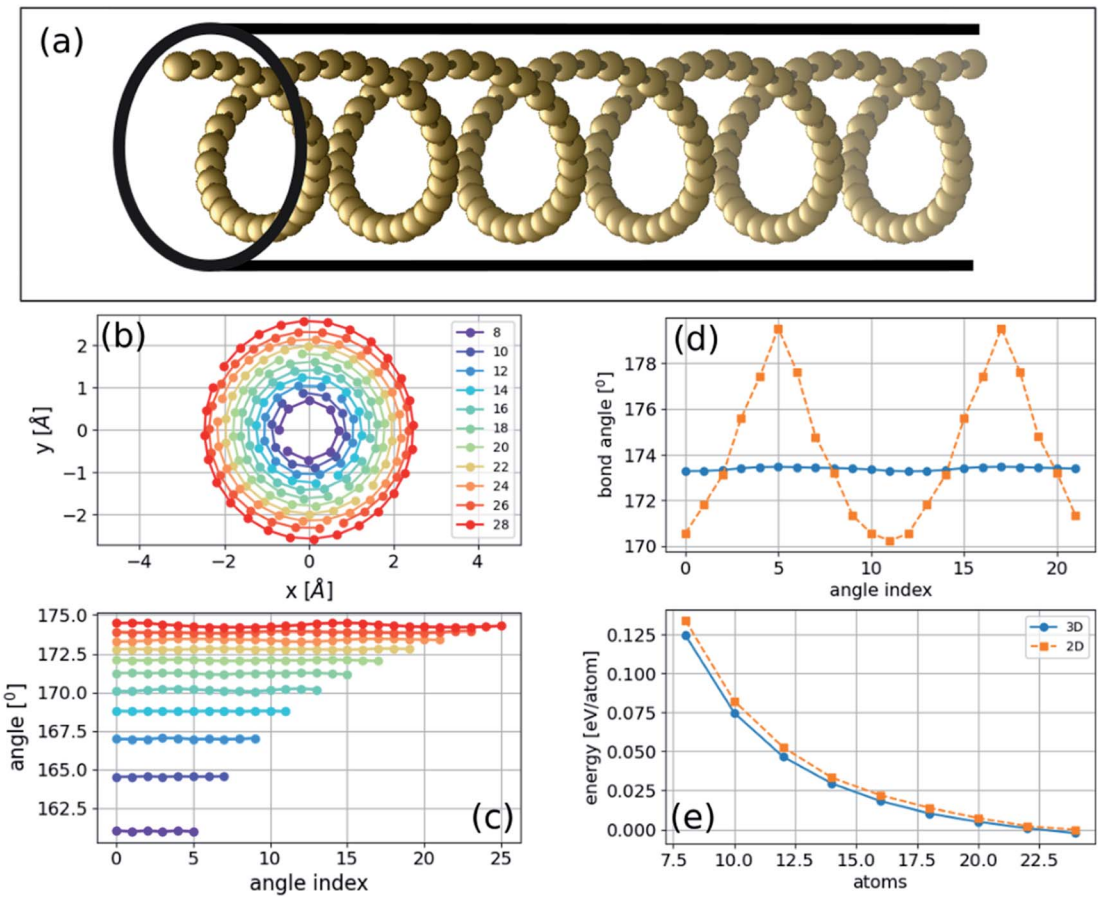

Fig. 3 Three-dimensional structure of a compressed carbyne at constant strain with PBC: (a) the geometry of the structure with black lines illustrating a CNT; (b) a projection of one cycle of the helical chain with the number of atoms in the unit cell in the legend; (c) bond angles for the three-dimensional structure; (d) comparison between the bond angles of the two- and three-dimensional structures; and (e) comparison of the total energy in the two- and three-dimensional structures.

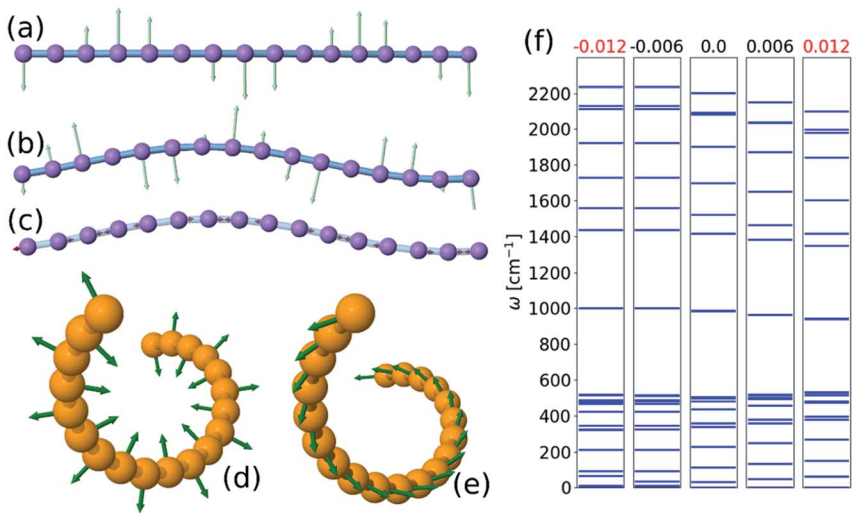

Fig. 4 Phonon normal modes of a two-dimensional 16-atom chain under −0.015 strain and three-dimensional 20-atom chain under 0.04 strain: (a) 10th mode with a frequency of 95 cm^{-1}; (b) 13th mode with a frequency of 212 cm^{-1}; (c) 41st mode with a frequency of 1728 cm^{-1}; (d) mode number 34; (e) mode number 4. (a)–(c) are two dimensional, and (d) and (e) are three dimensional; (a) is rotated 90° about the chain axis, and the vibrations are normal to the bending plane; the arrow lengths are the scaled displacements of each mode, and (f) Γ point phonon frequencies of a chain with a 16-atom unit cell.

the Γ point in 16-atom unit cells as a function of strain, and the results are presented in Fig. 4(f). The positive real frequencies indicate that the two-dimensional curved chain is dynamically stable. Transverse optical phonon mode frequencies decrease with strain, *i.e.*, they have negative-mode Grüneisen parameters, γ_ε, whereas the lower frequency longitudinal modes present a positive γ_ε. Furthermore, these trends are comparable to those found in the linear chain under tension, and similar results are obtained for the three-dimensional helical structure. Visualizations of selected phonon modes of the chain are shown in Fig. 4.

Atomistic model for the bent chain

To model carbyne chains under strain, we constructed the energy from a simple harmonic model with force constants (or springs) for each bond and bending constants for each bond angle to represent the three-body angular terms as follows:

$$E = \frac{1}{2}\sum_i c_i\left(L_i - L_i^0\right)^2 + \frac{1}{2}{L_0}^2\sum_i \xi_i {\alpha_i}^2, \quad (5)$$

where L_i is the bond length between atom i and atoms $i+1$, L_i^0 is the relaxed bond length between atom i and atoms $i+1$ (relaxed spring distance), L_0 is the average L_i^0, and α_i is the supplementary of the bond angle formed by three atoms centered on atom i measured in radians, *i.e.*, a measure of their deviation from a straight line. Both sums are over all the atoms in the chain, except the terminal atoms in finite chains. The parameters of this model are the force constants, c_i, the relaxed bond lengths, L_i^0, and the bending parameters, ξ_i. In the present definition, ξ_i has the same units as the force constants. The first term is the leading order in $(L_i - L_i^0)$, the harmonic term, and the second term is the leading order in α_i; thus, this model is a good approximation when $(L_i - L_i^0)$ and α_i are small. Similar models for the carbon chain were considered in ref. 10 and 18 and they are expected to be realistic because of the strong covalent bonds of carbon.

In the case of polyyne carbon chains, there are two force constants, c_1 and c_2, representing the alternating bonds and one bending parameter, ξ, whereas in cumulene chains there is only one force constant and one bending parameter. A parabolic fit of the energy can determine the force constants as a function of longitudinal atomic displacement in the absence of bending, in which just one bond is altered. This procedure can be computationally achieved using a four-atom unit cell: …C–C≡C–C. In which, either only the two central atoms adjacent to the triple bond are displaced, or only the two atoms at both ends are displaced. Such a calculation is performed for several strains, and the results are shown in Fig. 5. We found that the values of the force constants for the triple (hard) and single (soft) bonds are 80.5 and 63.9 eV Å^{-2}, respectively. Both force constants have a linear dependence on the strain with similar slopes of −547

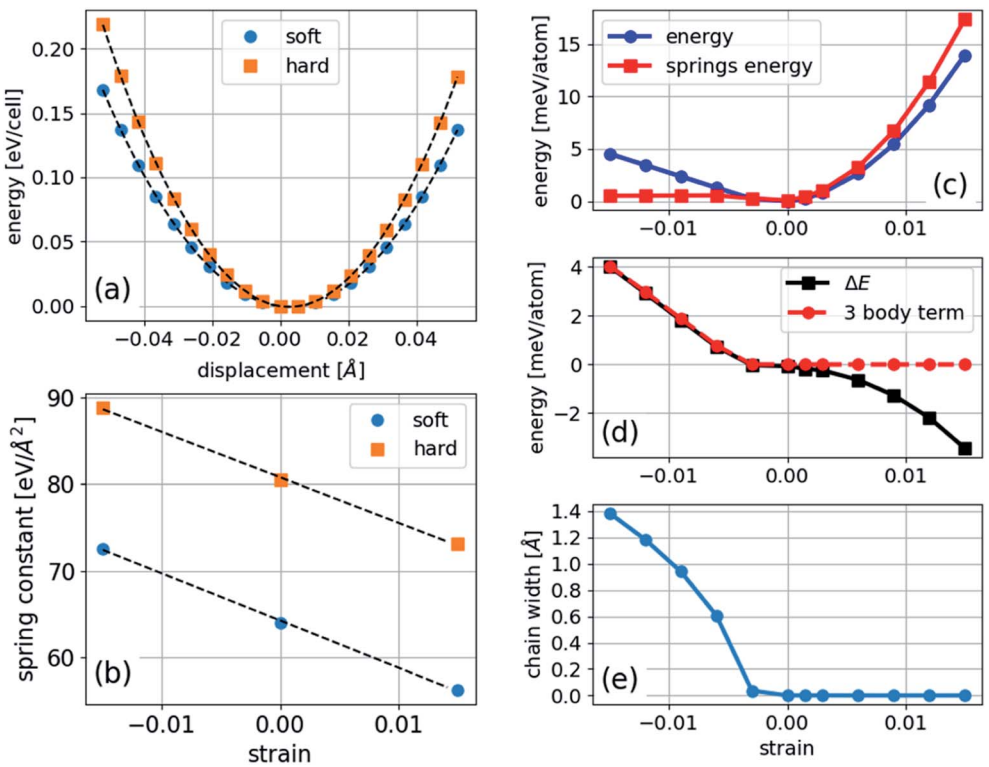

Fig. 5 Energy calculation for modeling: (a) energy as a function of displacement of one type of bond (the other bond is rigid) in a four-atom unit cell at zero strain with dashed lines, representing parabolic fits; (b) force constant calculation from the parabolic fit at several strains; (c) energy of the two-dimensional structure (through DFT) and harmonic energy calculated using the force constants; (d) difference between the energy, harmonic energy, and three-body term fitted to the negative strain region of the energy difference; and (e) chain width determined as the maximum distance between the atoms in the bending direction.

and −527 eV Å^{-2} for the soft and hard bonds, respectively. This result contradicts the assumption made in ref. 11 that only the soft bond force constant changes with pressure.

To determine the bending parameter, the difference between the calculated total energy and the modeled harmonic energy under compression is fitted to eqn (5), and the results are presented in Fig. 5. The anharmonic deviation present in a linear chain under compression (Fig. 5(c) and (d)) is much smaller in bending under compression because the bonds are nearly relaxed to their unstrained lengths. The value of ξ for the carbon nanochain is 1.56 eV Å^{-2}, which is approximately 45 times smaller than that of the average force constant, meaning that the chain is much softer toward bending than stretching. Our calculated value of ξ agrees with the value of 1.77 eV Å^{-2} calculated for finite carbon chains,[18] which validates the generality of this model.

Dispersion relation for the linear chain – analytical stability condition – infinite chains

The dispersion relation of the phonons in an infinite chain with two bond types is given as follows (see ESI† for full derivation):

$$m\omega^2 = \beta_1 + \beta_2 + 6\xi + 2\xi\cos(2k\Delta x) \pm \sqrt{(\beta_2 + \beta_1\cos(2k\Delta x) + 4\xi\cos(2k\Delta x) + 4\xi)^2 + (\beta_1\sin(2k\Delta x) + 4\xi\sin(2k\Delta x))^2} \quad (6)$$

where $\beta_i \equiv c_i\varepsilon$ is the effective force constant for transverse motion, ε is the strain, and $\Delta x = (1+\varepsilon)L_0$. The long-wavelength limit of the dispersion relation for this chain is:

$$m\omega^2 = \frac{2(\beta_1\beta_2 + 2\xi(\beta_1+\beta_2))}{\beta_1+\beta_2+8\xi}(k\Delta x)^2. \quad (7)$$

Both β_1 and β_2 are either positive, negative, or zero, as determined by the strain. At small compressive strains (negative β_1 and β_2), the long-wavelength limit exhibits instability with a negative numerator and positive denominator in eqn (7), yielding a bent chain. Thus, the infinite chain will not be stable under any compression. Moreover, the instability in this limit is also obtained in DFT calculations, as shown in Fig. 1.

For completeness, we also determine the dispersion relation for cumulenes, an infinite chain with one type of bond. The dispersion relation of the transverse acoustic branch of this chain is (see ESI†):

$$m\omega^2 = 2\beta + 6\xi - 2(\beta + 4\xi)\cos(\Delta x \times k) + 2\xi\cos(2\Delta x \times k), \quad (8)$$

where $\beta = \beta_1 = \beta_2$. In the long-wavelength limit, this dispersion relation becomes

$$\omega = \left(\sqrt{\frac{2\beta}{m}}\Delta x\right)k. \quad (9)$$

Thus, similar to a chain with two types of bonds, this infinite linear chain is not stable under any compression, and the frequency becomes imaginary when $\Delta x < L_0$. In the long-wavelength limit, where instability is present, the bending term has no effect because ω does not depend on ξ.

At zero strain, the linear term vanishes, the sound velocity is zero, and the transverse acoustic branch has a nonlinear shape (non-Debye form) similar to the acoustic branch of graphene (Fig. 6(a)). To obtain the long-wavelength limit under these conditions, we expand eqn (8) to the fourth-order in $\Delta x \times k$ as follows:

$$m\omega^2 = \beta(\Delta x \times k)^2 - \frac{1}{12}\beta(\Delta x \times k)^4 + \xi(\Delta x \times k)^4, \quad (10)$$

where the first two terms vanish at zero strain and ω has a parabolic dependence on k.

To see the effect of the bending term on stabilizing the finite linear chain under strain to the leading order, we use the expansion of ω^2 to the fourth-order in eqn (10). Within this approximation, the condition for stability for a given value of k is

$$\varepsilon > -\frac{\alpha}{\alpha+1}, \quad (11)$$

where

$$\alpha = \frac{\xi}{c}\frac{(\Delta x \times k)^2}{\left(1 - \frac{1}{12}(\Delta x \times k)^2\right)}, \quad (12)$$

is a dimensionless constant. A similar condition can be found for polyyne, as the expansion of ω^2 also has the form $m\omega^2 = \eta_1(\Delta x \times k)^2 + \eta_2(\Delta x \times k)^4$ where η_1 and η_2 are parameters that depend on β_1, β_2 and ξ as in eqn (10), which are reported in the ESI.†

The instability of an infinite chain with increasing compression is illustrated in Fig. 6(a). As the bending parameter ξ increases relative to the force constant c, for example, in other materials, the chains become more stable (Fig. 6(b)). If $\xi = 0$, the chain is not stable with respect to any transverse displacement under compression because the harmonic term is determined only by the distances between the atoms.

The equations of motion for finite and infinite chains are the same, whereas their boundary conditions are different. Thus, we can apply the dispersion relation of an infinite chain to a finite chain by selecting only discrete values of the wavevector, k, to obtain the discrete normal modes of the finite chain.

Applying the boundary conditions of a standing wave, the allowed values of k are given by the following relation:

$$k_m = \frac{\pi}{\Delta x}\frac{m}{(N-1)}, \quad (13)$$

where N is the number of atoms in the chain and $m < N - 1$ is the normal mode index. The stability of a finite chain is

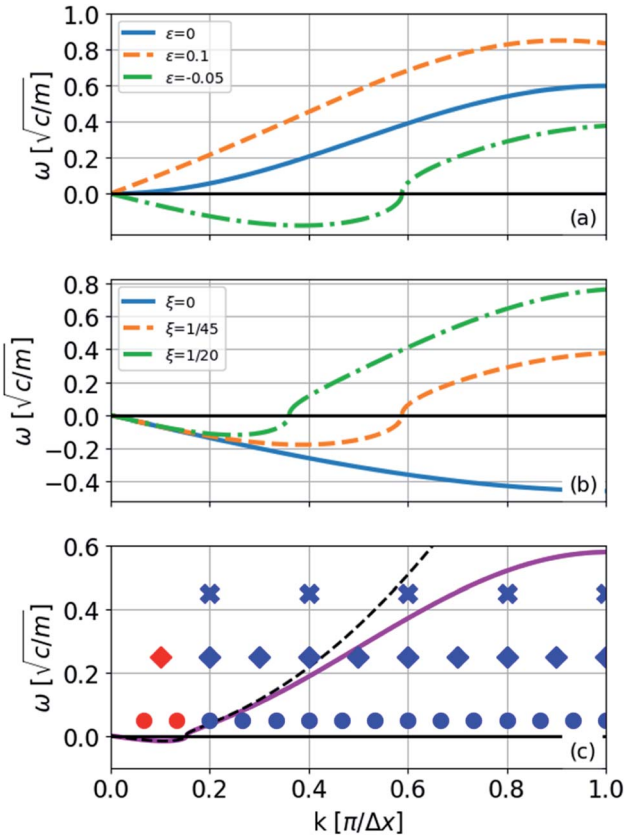

Fig. 6 Phonon spectrum of the transverse normal mode (eqn (8)) of the model represented in eqn (5) with one type of bond: (a) $\xi = (1/45)c$ with different strains indicated in the legend; (b) a strain of -0.05 and different values of ξ in units of c; (c) a strain of -0.005; the dashed line is ω approximated by a fourth-order expansion of ω^2, the solid line is the exact expression, and the markers are the k-levels for 6-, 11-, and 16-atom chains from top to bottom (eqn (13)).

analyzed in Fig. 6(c), where the fourth-order expansion is shown to be a good approximation for the dispersion relation. The discrete k-levels are shown with markers. For the 16- and 11-atom chains, the frequencies of the lowest k-levels are imaginary. For example, if we consider an 11-atom carbon chain, the condition for stability is a strain of -0.2%. However, for a 6-atom chain, all the frequencies are real for all the k-levels, representing a stable structure.

The condition for stability is that all the frequencies are real. Because the imaginary frequencies of the transverse acoustic branch are present in the long wavelength limit (as explained above and shown in Fig. 6), the condition for stability is that the smallest positive allowed value of k ($m = 1$ in eqn (13)) has a real frequency. From this consideration and eqn (12), we obtain

$$\alpha = \frac{\xi}{c}\frac{(\pi/(N-1))^2}{\left(1-\frac{1}{12}(\pi/(N-1))^2\right)}. \quad (14)$$

In the limiting case where $\alpha = 0$, which occurs if there is no resistance to bending ($\xi = 0$), the condition for stability is $\varepsilon > 0$. In real chains where $\xi \neq 0$, α is determined by the length of the chain, N, and the chain can be stably compressed with a negative ε up to a threshold value of $-\alpha/(\alpha + 1)$. This result means that compressed, finite, linear chains are stable if the strain is small enough and the chain is short enough.

The atomistic model solution

The polyyne carbon–chain bending model presented in eqn (5) with two force constants and one bending parameter under a constant strain of -0.04 is numerically solved for finite chains of varying lengths. A gradient-based minimization algorithm is applied to minimize the energy in two and three dimensions. The results are presented in Fig. 7. A helical structure is obtained, as can be seen in Fig. 7(e) and (f). In the limit of long chains, the MBA approaches 180°, and the MBD approaches the mean relaxed bond distance, as shown in Fig. 7(b)–(d). Furthermore, the amplitude increases linearly with chain length at constant strain (Fig. 7(d)).

The energies of the three-dimensional structures are slightly lower than those of the two-dimensional structures, consistent with the *ab initio* results (Fig. 7(a)). Moreover, the most significant contribution to the energy was the angular component (the second term in eqn (5)). As the angles were approximately constant in the three-dimensional structure and varied in the two-dimensional structure (Fig. 4(d) and similar results obtained from the analytical model below), we conclude that the lower energy in the three-dimensional structure is determined by the constant angle distribution that cannot be achieved in two dimensions.

Continuum approach

The stationary structures of carbon chains under compression can be described in a continuum model, similar to an elastic rod. In this approach, we consider harmonic and bending forces derived from the two terms in eqn (5), which act on an infinitesimal length of the chain. These two forces have opposite signs that cancel each other out at mechanical equilibrium as follows:

$$\frac{T_o d^2y}{dx^2} = {L_0}^3 \xi \frac{d^4y}{dx^4}, \quad (15)$$

where $T_0 = c\Delta L$ is the tension, which is negative under compression. This equation is identical to that obtained for an elastic rod:[21]

$$IE\frac{d^4y}{dx^4} = T\frac{d^2y}{dx^2}, \quad (16)$$

Consequently, we can identify the atomic bending parameter ${\xi L_0}^3$ with the continuum product of the moment of inertia, I, and Young's modulus, E. This analogy resolves an ongoing controversy over the value of Young's modulus in carbon chains. Comparing the two equations shows that the question is undefined and that atomistic properties are determined by the product IE and not *via* Young's modulus by itself. This problem leads to the wide range of values, between 0.3 and 32.7 GPa for Young's modulus, as mentioned in the introduction, because

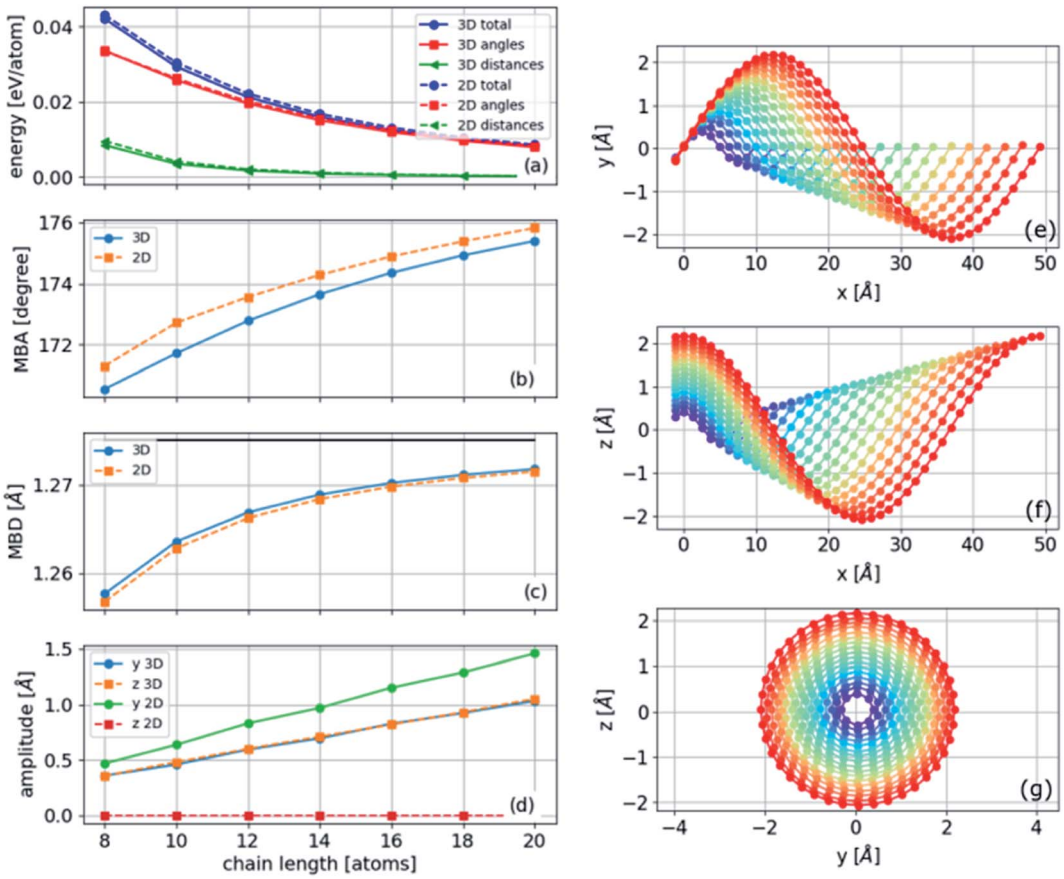

Fig. 7 Left panel: comparison between two- and three-dimensional structures: (a) total and individual components of energy; (b) mean bond angle (MBA); (c) mean bond distance (MBD), with the black solid line as the mean relaxed bond distance; (d) amplitudes along each direction. Right panel: atomic positions of the three-dimensional structure where x is the periodic direction; all calculations are under −0.04 strain with PBC.

different calculations make different assumptions regarding the cross section of the nanowire, which is not a well-defined quantity.

The equilibrium equation can be transformed to yield a wave equation (ESI† for the derivation):

$$\frac{\partial^2 \psi_j}{\partial x^2} = \left(\frac{c\Delta L}{\xi {L_0}^3}\right)\psi_j = \left(\frac{T_0}{\xi {L_0}^3}\right)\psi_j; \quad T_0 = c\Delta L, \tag{17}$$

where $\psi_j = \Delta x \times \partial {r_j}^2/\partial x^2$ is the bond angle in the xy or xz planes, $r_j = y, z$, or equivalently the curvature of the chain in the continuum limit. $\Delta L = |L_i - L_i^0|$ is the bond distance contraction, which we assume is equal for all atomic pairs.

This wave equation is an eigenvalue equation where the eigenvalues and eigenfunctions determine the geometry of the chain by the compression parameter ΔL and the curvatures, respectively. This equation can also describe a dimerized chain where c is the average value of the spring constants (more details below).

This equation can describe both two- and three-dimensional structures. In two dimensions, it is analogous to the time-independent Schrödinger equation for a free particle. However, in three-dimensions, the eigenvalues along the y and z directions are restricted to be the same because they are both determined by the tension, unlike the Schrödinger equation for a free particle. Consequently, the periods in both directions are equal.

The solutions of the wave equation in two-dimensions, similar to a particle in a box, are

$$\psi(x) = A\ sin(kx + \phi), \tag{18}$$

and in three dimensions:

$$\psi_y(x) = A\ \sin(kx), \tag{19}$$

$$\psi_z(x) = A\ \sin(kx + \phi),\ \phi \neq 0. \tag{20}$$

In PBC, with $\psi_j(x = 0) = \psi_j(x = N\Delta x)$ and $\psi_{j'}(x = 0) = \psi_{j'}(x = N\Delta x)$, representing an infinite chain, only an integer number of periods is allowed ($n = 1, 2, 3,\ldots$). This wave equation indicates that at a fixed compression, there exist excited configurational states of the chain, $n > 1$, commonly referred to as metastable states.

In finite boundary conditions (FBC), with $\psi_j(x = 0) = 0$ and $\psi_j(x = N\Delta x) = 0$, representing a finite, free chain, an integer number of half periods ($n = 1/2, 1, 3/2,\ldots$) is allowed for the two-dimensional structures. In the three-dimensional case, the

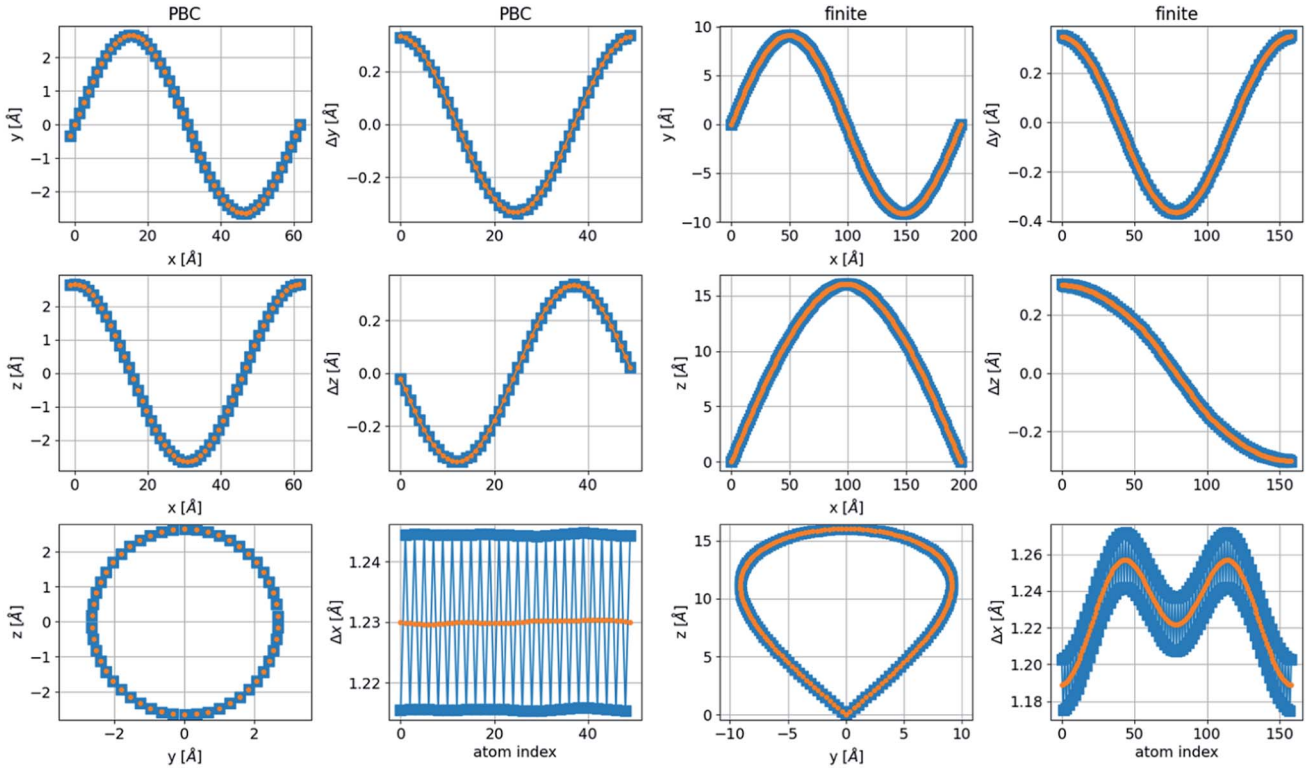

Fig. 8 Geometry of the chain for lowest-energy three-dimensional structures with PBC and FBC for chains with (blue squares) and without (orange circles) dimerization. The PBC structure has $n = 1$ in both directions, and the FBC structure has $n = 1$ in the y-direction and $n = 1/2$ in the z-direction, a nonequal period structure. Without dimerization, the spring distance is constant for all springs, 1.2746 Å, and the relaxed spring distance is 1.275 Å. With dimerization, the distances are 1.2595 Å and 1.2896 Å, and the relaxed distances are 1.26 Å and 1.29 Å, respectively. The spring constant in the structure without dimerization is the average of the two spring constants used in the structures with dimerization. All parameters are taken from the DFT calculations.

additional boundary condition is $\psi_{j'}(x = 0) = \psi_{j'}(x = N\Delta x) \neq 0$, where $j' \neq j$, which allows only an integer number of periods in the additional dimension. Thus, the ground state of the finite three-dimensional chain corresponds to $n = 1/2$ in one transverse dimension and $n' = 1$ in the other transverse dimension. This structure has a nonequal x separation to create a bond length very close to the relaxed distance, as shown in Fig. 8, together with a geometrical description of a chain in PBC. This structure with unequal periods has a noncircular cross-section.

The bent chain structures are stabilized mainly by the energy of the bond force constants. Thus, the bond length $L_i = \sqrt{\Delta x^2 + \Delta y^2 + \Delta z^2}$ is very close to the relaxed value, L_0, and where Δy and Δz are approximately proportional to the derivatives dy/dx and dz/dx (exactly proportional where Δx is constant), respectively, as shown in Fig. 8. In the case where the periods are the same along both the y and z directions with a $\pi/2$ phase difference, $y(x) = A\sin(kx)$, $z(x) = A\cos(kx)$, and $\Delta y^2 + \Delta z^2 = A^2$. Then both Δx and $L_i = \sqrt{\Delta x^2 + A^2}$ are constant. However, in a structure with unequal periods, $\Delta y^2 + \Delta z^2$ is no longer constant. Since L_i remains constant from the same considerations, Δx cannot be constant, as shown in Fig. 8. Although the dimerization of the polyyne structures cannot be directly inserted into the wave equation, taking the average of the force constants and relaxed distances is a valid approach, as shown in Fig. 8.

We assume that the solutions to the wave equation[14] increase in energy with an increasing number of periods, n. To establish this assumption, we calculate the energy explicitly by the following procedure: (1) PBC or FBC determine the discrete wavenumber k, (2) substitute eqn (18) or (19) and (20) into eqn (17) to obtain ΔL (from the substitution of eqn (19) and (20) in (17) we obtain the same ΔL), and (3) calculate the two contributions of the energy using eqn (5) with the continuum approach (ESI†). These two contributions are

$$E_n^{\text{springs}} = E_1^{\text{springs}} n^4, \tag{21}$$

$$E_n^{\text{bending}} = E_1^{\text{bending}} n^2, \tag{22}$$

where the total energy is the sum (ESI† for the full derivation).

The energy can also be obtained numerically from the atomistic model. Thus, we validate the results for the energy, as shown in Fig. 9. Under FBC, the lowest-energy two-dimensional structure has $n = 1/2$, while in three dimensions, $n = 1$ in one transverse dimension and $n = 1/2$ in the other. Thus, the ground state of a finite chain under compression is a two-dimensional arc-shaped structure.

The ground state under FBC of the chain is an arc-shaped two-dimensional structure ($n = 1/2$), and therefore it is the most probable structure to obtain in an experiment. The

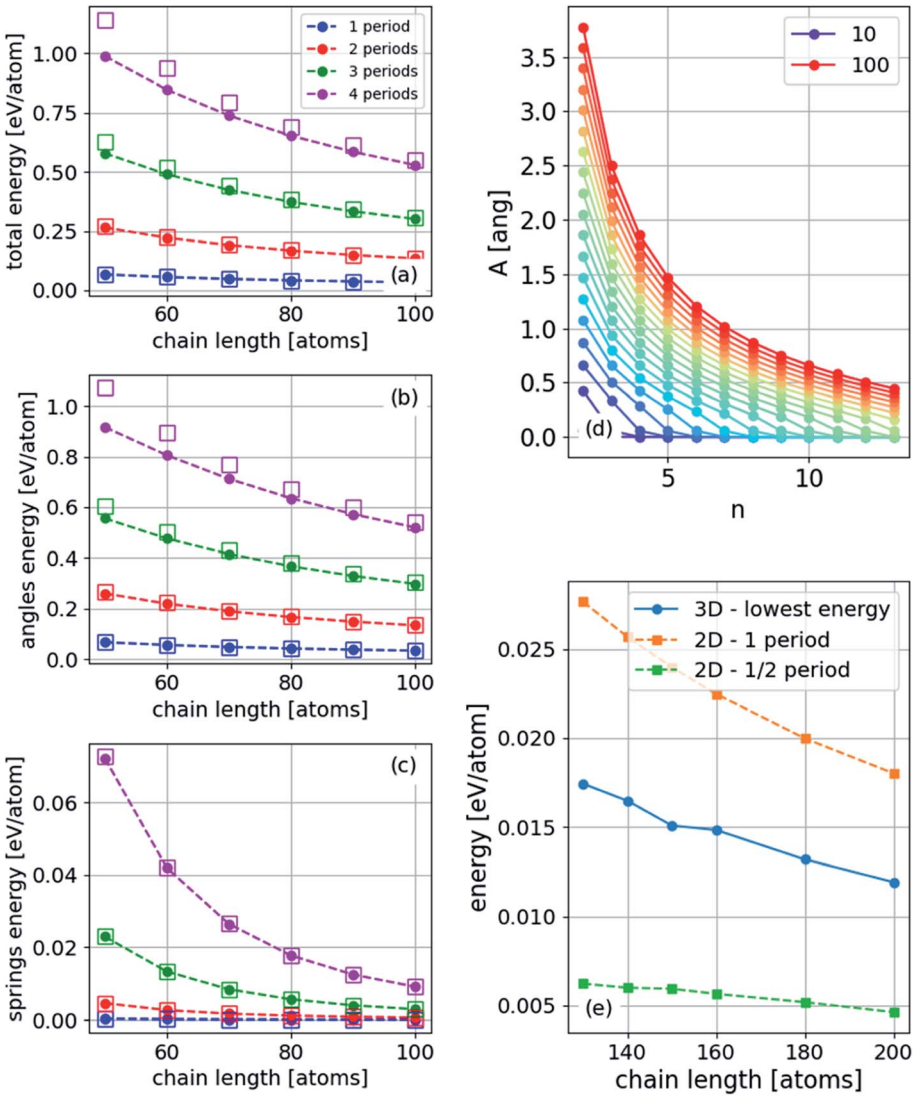

Fig. 9 (a) Total, (b) angle (bending), and (c) harmonic energy for three-dimensional structures with PBC for different numbers of periods (wavelengths) in the unit-cell. The squares are determined using eqn (21) and (22), where E_1^{springs} and E_1^{bending} were obtained from the energies of a single period. (d) Amplitude, A, for PBC for different chain lengths indicated in the legend (atoms) and different excited states, n, and (e) energy for a finite chain: two lowest energy states for two-dimensional structure and the lowest three-dimensional structure (the geometry of this structure is shown in Fig. 10).

nonequal periods' three-dimensional structure ($n = 1/2$ along y and $n = 1$ along z) is the first excited state. However, the energy difference depends on the length of the chain and on the strain. As the chains become longer and the strain becomes smaller, the energy difference decreases as shown in Fig. 7. Furthermore, in the high excited states, at constant strain, the amplitude is considerably smaller, as shown in Fig. 9(d).

Under compression, the CNT can remain straight or it can collapse. This buckling depends on the diameter of the CNT and the number of walls[22,23] and is affected by the presence of chain filling.[24,25] Here we consider the case in which the CNTs remain straight. Where the carbon chain is confined in a CNT (Fig. 4), the amplitude is constrained to be smaller than the CNT's radius. Under sufficient compression, the amplitude of the arc of the bent carbon chain becomes larger than the diameter of the tube. Thus, the carbon chain must be in one of the excited states—either in three- or two dimensions. The first accessible states with increasing deformation are the excited states of the 2D sine with shorter periodicities. However, after two or three such excitations another alternative emerges and that is the formation of a helix structure with a longer period, *i.e.* in a lower excited state, but with the same strain. Further compression requires that the chain occupy higher excited configurational states, thus increasing the number of contact points with the CNT.

As a concrete example we present a calculation of the diameter of the 2D sine-wave and the 3D helix structures as a function of the period length and strain in a CNT with 0.7 nm diameter (Fig. 10). At −0.02 strain the diameter of the 2D sine reaches the CNT diameter and therefore the period must

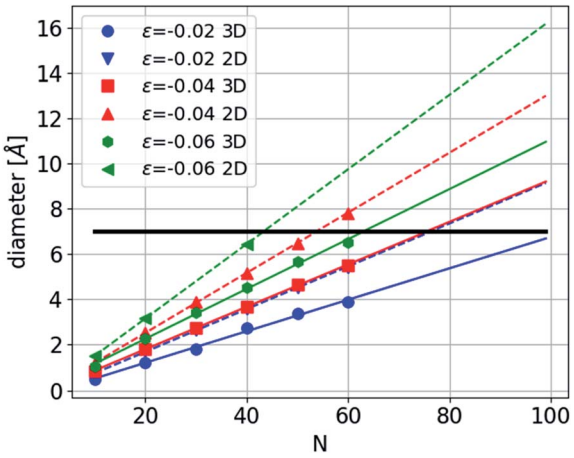

Fig. 10 The diameter of two- and three-dimensional ground states of long chains, using PBC, as a function of the number of atoms in the period of the chain, N, and the chain strain, ε, indicated in the legend. The solid and dashed lines are linear fits to the three- and two-dimensional diameters, respectively. The black solid line is a typical diameter of CNT. This calculation was obtained from the analytical model in the text.

decrease. At approximately half the period the 2D structure can continue until a strain of 0.04. At this point an alternative may be considered, the 3D helix with the same strain but a longer period by approximately 50%. The energy of this structure will be lower than that of the 2D structure as can be seen from the results above in Fig. 7. Of course, in an experimental situation the strain might be constrained because of the technical details of the experiments, like solidification of the pressure transmitting medium and the axial elastic modulus of the CNT. However, large strains of the carbon chain in the CNT can still be achieved through bending.

Charge transfer

If the carbon chain is linear at a sufficiently small length and strain, the frequency of the optical modes increases with increasing compression, as shown in Fig. 1. The high-frequency modes do not anomalously decrease with compression if the chain is bent, as shown in Fig. 4. Thus, the Raman anomaly observed experimentally in carbon nanowires encapsulated inside CNTs under compression cannot be explained by a force constant model of the nanowire (like the models introduced in ref. 11).

However, an alternative explanation is charge transfer between the CNT and the wire. It has been shown that in linear carbon wires encapsulated inside CNTs, charge transfers from the CNT to the wire and reduces the Raman frequency.[7] Furthermore, charge transfer was found in other systems between the molecular fillers and the CNTs.[26,27]

Under compression, it is reasonable that more charge will transfer to the nanowire because it becomes wider (more bent). Thus, the effect of charge transfer in chains under compression is examined with respect to both structural relaxation and phonon calculations, and the results are presented in Fig. 11. For simplicity, we only consider the two-dimensional structure. Similar to linear chains, we found that phonon frequencies decrease as the charge is transferred to the chain. This reduction is because of (i) the change in the lattice parameter, as

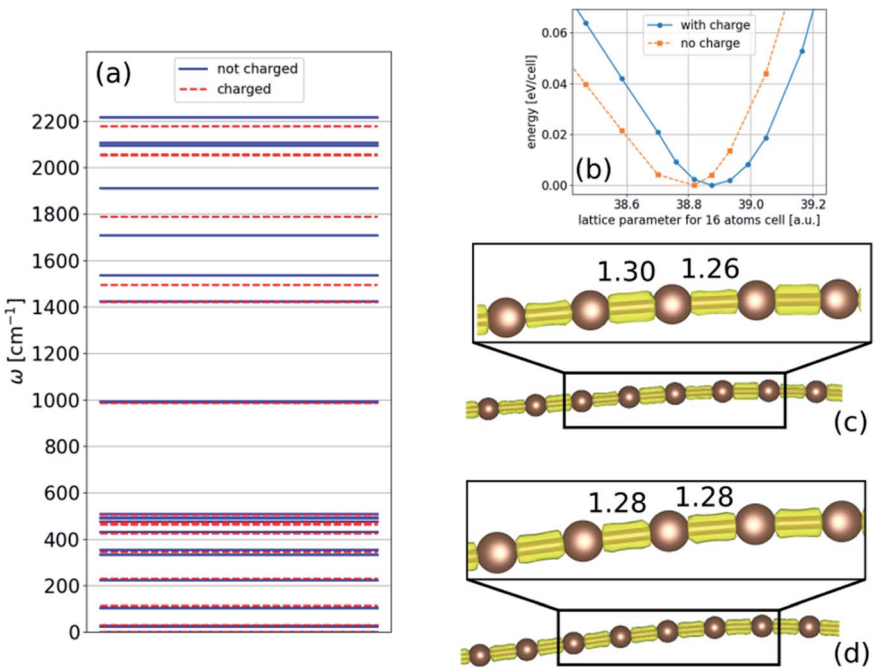

Fig. 11 Phonons and chain geometry calculation for a two-dimensional infinite chain with a 16-atom unit cell under compression with and without an extra electron: (a) phonon frequencies; (b) cold curve; (c) and (d) are chain geometry with and without charge, respectively; numbers indicate the bond length in Å

shown in Fig. 11(b), and (ii) the reduction in the BLA, which can reach the polyyne–cumulene transition, as shown in Fig. 11(c) and (d). These results suggest that the decrease in frequency may continue until the polyynes–cumulenes transition.

Conclusions

We found that an infinite linear chain is not stable under any compression using both *ab initio* calculations and an atomistic model. This instability results in new structures having two configurations: a two-dimensional sine-like shape and a three-dimensional helical structure. The ground-state is a two-dimensional structure in FBC and three-dimensional in PBC. Furthermore, we found meta-stable structures which are similar to the ground-state structures with shorter wavelengths. These structures can be described in a continuum formulation using a wave equation that also reveals the existence of excited configurational states (meta-stable states), which can be attained in experiments in which the carbon chain is confined inside a CNT. This wave equation can also be used in other systems if the atomic interactions can be described with two- and three-body terms. The wave equation formulation also indicates that the concept of Young's modulus for one-dimensional chains is ill-defined, thus explaining the wide range of values proposed. The BLA reaches a constant value as a function of compression strain, and the polyyne–cumulene transition does not occur because of bending (neglecting the effects of the environment on the chain). The bond force constants determine the chain's resistance to strain under tension and the bending constants when under compression. However, finite linear chains can be stable under small compressions if the chain is sufficiently short. Based on the above results, we have demonstrated that the proposed explanation of the Raman anomaly based on the softening of the harmonic force constant model in the case of a linear chain[11] is not valid. Furthermore, the Raman frequency does not decrease with the increasing compression of a bent chain. For carbon chains confined in CNTs, we suggest that the chain occupies periodic excited configurations under compression, increasing the contact between the chain and the CNT. Furthermore, a charge transfer from the CNT to the chain reduces the phonon frequency in both linear and bent chains and is most likely the mechanism responsible for the observed Raman anomaly.

Methods

First-principles based DFT calculations were performed using the plane-wave pseudopotential method in the Quantum Espresso simulation package.[28] The chains were modeled using a unit cell with periodic boundary conditions (PBC) along the chain and with vacuum spacing in two dimensions normal to the chain or three dimensions in the case of finite chains. Ultrasoft pseudopotentials from the GBRV set[29] and GGA-PBE exchange–correlation energy function were employed.[30] The number of *k*-points in the periodic direction in a two-atom unit cell was 40. In large supercells, this number was reduced inversely proportional to the increased cell size. The cutoff energies were 40 Ry for the plane-wave expansion of the wave function and 200 Ry for the density and potential functions. Phonons were calculated within the density-functional-perturbation theory approach,[31] as implemented in the Quantum Espresso package.

Conflicts of interest

There are no conflicts to declare.

References

1 J. A. Januszewski and R. R. Tykwinski, Synthesis and properties of long [*n*]cumulenes, *Chem. Soc. Rev.*, 2014, **43**, 3184.
2 A. Milani, *et al.*, Semiconductor-to-Metal Transition in Carbon-Atom Wires Driven by sp^2 Conjugated End Groups, *J. Phys. Chem. C*, 2017, **121**, 10562–10570.
3 K. Zhang, Y. Zhang and S. Shi, A review of linear carbon chains, *Chin. Chem. Lett.*, 2020, **31**, 1746–1756.
4 E. Buntov, *et al.*, Structure and Properties of Chained Carbon: Recent *Ab Initio* Studies, *C—J. Carbon Res.*, 2019, **5**, 56.
5 C. S. Casari and A. Milani, Carbyne: from the elusive allotrope to stable carbon atom wires, *MRS Commun.*, 2018, **8**, 207–219.
6 S. Heeg, *et al.*, Carbon Nanotube Chirality Determines Properties of Encapsulated Linear Carbon Chain, *Nano Lett.*, 2018, **18**, 5426–5431.
7 M. Wanko, *et al.*, Polyyne electronic and vibrational properties under environmental interactions, *Phys. Rev. B*, 2016, **94**, 195422.
8 U. Argaman, D. Kartoon and G. Makov, Driving forces behind the distortion of one-dimensional monatomic chains: Peierls theorem revisited, *Phys. Rev. B*, 2018, **98**, 165429.
9 V. I. Artyukhov, M. Liu and B. I. Ya, Mechanically Induced Metal−Insulator Transition in Carbyne, *Nano Lett.*, 2014, **14**, 4224–4229.
10 I. E. Castelli, P. Salvestrini and N. Manini, Mechanical properties of carbynes investigated by *ab initio* total-energy calculations, *Phys. Rev. B: Condens. Matter Mater. Phys.*, 2012, **85**, 214110.
11 K. Sharma, *et al.*, Anharmonicity and Universal Response of Linear Carbon Chain Mechanical Properties, *Phys. Rev. Lett.*, 2020, **125**, 105501.
12 M. Liu, *et al.*, Carbyne from First Principles: Chain of C Atoms, a Nanorod or a Nanorope, *ACS Nano*, 2013, **7**(11), 10075–10082.
13 A. Milani, *et al.*, First-principles calculation of the Peierls distortion in an infinite linear carbon chain: the contribution of Raman spectroscopy, *J. Raman Spectrosc.*, 2008, **39**, 164–168.
14 Md. M. Haque, *et al.*, Vibrational and NMR properties of polyynes, *Carbon*, 2011, **49**, 3340–3345.
15 W. Q. Neves, *et al.*, Effects of pressure on the structural and electronic properties of linear carbon chains encapsulated in double wall carbon nanotubes, *Carbon*, 2018, **133**, 446–456.

16 N. F. Andrade, A. L. Aguiar, Y. A. Kim, M. Endo, P. T. C. Freire, G. Brunetto, D. S. Galvao, M. S. Dresselhaus and A. G. Souza Filho, Linear Carbon Chains under High-Pressure Conditions, *J. Phys. Chem. C*, 2015, **119**(19), 10669–10676.
17 A. Lucotti, *et al.*, Evidence for Solution-State Nonlinearity of sp-Carbon Chains Based on IR and Raman Spectroscopy: Violation of Mutual Exclusion, *J. Am. Chem. Soc.*, 2009, **131**, 4239–4244.
18 Y. H. Hu, Bending Effect of sp-Hybridized Carbon (Carbyne) Chains on Their Structures and Properties, *J. Phys. Chem. C*, 2011, **115**, 1843–1850.
19 A. Lucotti, *et al.*, Bent polyynes: ring geometry studied by Raman and IR spectroscopy, *J. Raman Spectrosc.*, 2012, **43**, 95–101.
20 X. Fan, *et al.*, Atomic Arrangement of Iodine Atoms inside Single-Walled Carbon Nanotubes, *Phys. Rev. Lett.*, 2000, **84**(20), 4621.
21 L. D. Landau and E. M. Lifshitz, *Course of Theoretical Physics Vol 7: Theory and Elasticity*, Pergamon Press, 1959.
22 Y. Magnin, *et al.*, Collapse phase diagram of carbon nanotubes with arbitrary number of walls. Collapse modes and macroscopic analog, *Carbon*, 2021, **178**, 552–562.
23 T. F. T. Cerqueira, Density-functional tight-binding study of the collapse of carbon nanotubes under hydrostatic pressure, *Carbon*, 2014, **69**, 355–360.
24 C. Bousige, *et al.*, Superior carbon nanotube stability by molecular filling:a single chirality study at extreme pressures, *Carbon*, 2021, **183**, 884–892.
25 A. C. Torres-Dias, *et al.*, Chirality-dependent mechanical response of empty and water-filled single-wall carbon nanotubes at high pressure, *Carbon*, 2015, **95**, 442–451.
26 R. S. Alencar, Raman resonance tuning of quaterthiophene in filled carbon nanotubes at high pressures, *Carbon*, 2021, **173**, 163–173.
27 L. Alvarez, *et al.*, High-pressure behavior of polyiodides confined into single-walled carbon nanotubes: A Raman study, *Phys. Rev. B: Condens. Matter Mater. Phys.*, 2010, **82**, 205403.
28 P. Giannozzi, *et al.*, QUANTUM ESPRESSO: a modular and open-source software project for quantum simulations of materials, *J. Phys.: Condens. Matter*, 2009, **21**, 395502.
29 K. F. Garrity, *et al.*, Pseudopotentials for high-throughput DFT calculations, *Comput. Mater. Sci.*, 2014, **81**, 446.
30 J. P. Perdew, K. Burke and M. Ernzerhof, Generalized Gradient Approximation Made Simple, *Phys. Rev. Lett.*, 1996, **77**, 3865.
31 S. Baroni, *et al.*, Phonons and related crystal properties from density-functional perturbation theory, *Rev. Mod. Phys.*, 2001, **73**, 515.